جامعة القاهرة

Department of Electronics and Electrical Communications Engineering

Faculty of Engineering - Cairo University

ELC 3050 Project

Design a 2-element array of dual-band microstrip patch antenna operating at 15 and 30 GHz

Under Supervision of Prof.: Islam A. Eshrah & Eng. Mohamed Khaled

Name	Section	ID	BN
شهاب الدين طارق فؤاد محمد علي	2	9220392	24
محمود تامر على على على غضنفر	3	9220774	36
محمود سعيد غمرى مصطفى	3	9231950	37
محمد خالد فتحى محمد ربيع	3	9220684	24
محمد احمد محمد السيد	3	9220653	19
محمد احمد محمد احمد الهجين	3	9220652	18

Table of Contents

Table of Figures

1. Framework:

1.1 Introduction:

This report presents the design, simulation, and measurement of a novel 2-element dual-band microstrip patch antenna operating at **15 GHz** and **30 GHz**.

The antenna utilizes **Edge Feeded Slotted Patch** to achieve dual-band operation. The design process involved defining the design specifications, conducting electromagnetic simulations using **HFSS** and refining the design iteratively based on the simulation results. A prototype of the antenna was fabricated on a **FR4** substrate. The fabricated antenna was characterized by measuring its S-parameters ,Radiation Patterns, Gain, Input Impedance.

The measured results demonstrated good agreement with the simulated results with The operating Bandwidths, S-parameters ,Radiation Patterns, Gain, Input Impedance within acceptable limits. This work demonstrates the feasibility of designing compact and efficient dual-band microstrip patch antennas for applications in 5G and Beyond Wireless Communication , Satellite Communication , Radar Systems , Radio Astronomy and Remote Sensing.

1.2 Problem Definition:

This research investigates the design and development of a compact and efficient dual-band microstrip patch antenna operating at 15 GHz and 30 GHz. The primary challenge lies in achieving independent resonances at both frequencies while maintaining acceptable bandwidth, gain, and impedance matching. Additionally, the design must consider practical constraints such as fabrication limitations and desired radiation characteristics.

1.2.1 Dual band MSP :

The primary challenge lies in designing a microstrip patch antenna capable of efficient operation at two distinct frequency bands (15 GHz and 30 GHz). This necessitates careful consideration of the following:

- **Multi-Resonance**: Achieving simultaneous and independent resonances at both frequencies while maintaining adequate bandwidth and impedance matching at each band.
- **Design Techniques**: Exploring and implementing suitable design techniques such as slotted patches, parasitic elements, or multi-layered structures to achieve the desired dual-band operation.
- **Performance Optimization**: Optimizing the antenna geometry, dimensions, and substrate parameters to achieve the desired radiation characteristics, including gain, efficiency, and radiation patterns.

1.2.2 2-Element Antenna Array:

Integrating two dual-band MSPs into an array introduces additional design considerations:

- **Mutual Coupling**: Minimizing mutual coupling effects between the two elements to ensure independent operation and prevent performance degradation of each element.
- **Array Configuration**: Determining the optimal array geometry (e.g., linear, planar) and element spacing to achieve desired radiation patterns and array factor characteristics.
- **Feeding Network**: Designing an efficient feeding network to provide appropriate excitation to each element in the array while minimizing losses and maintaining impedance matching.

2. Design Procedure :

2.1 Rectangular Edge fed microstrip patch antenna with slots - based design [1]:

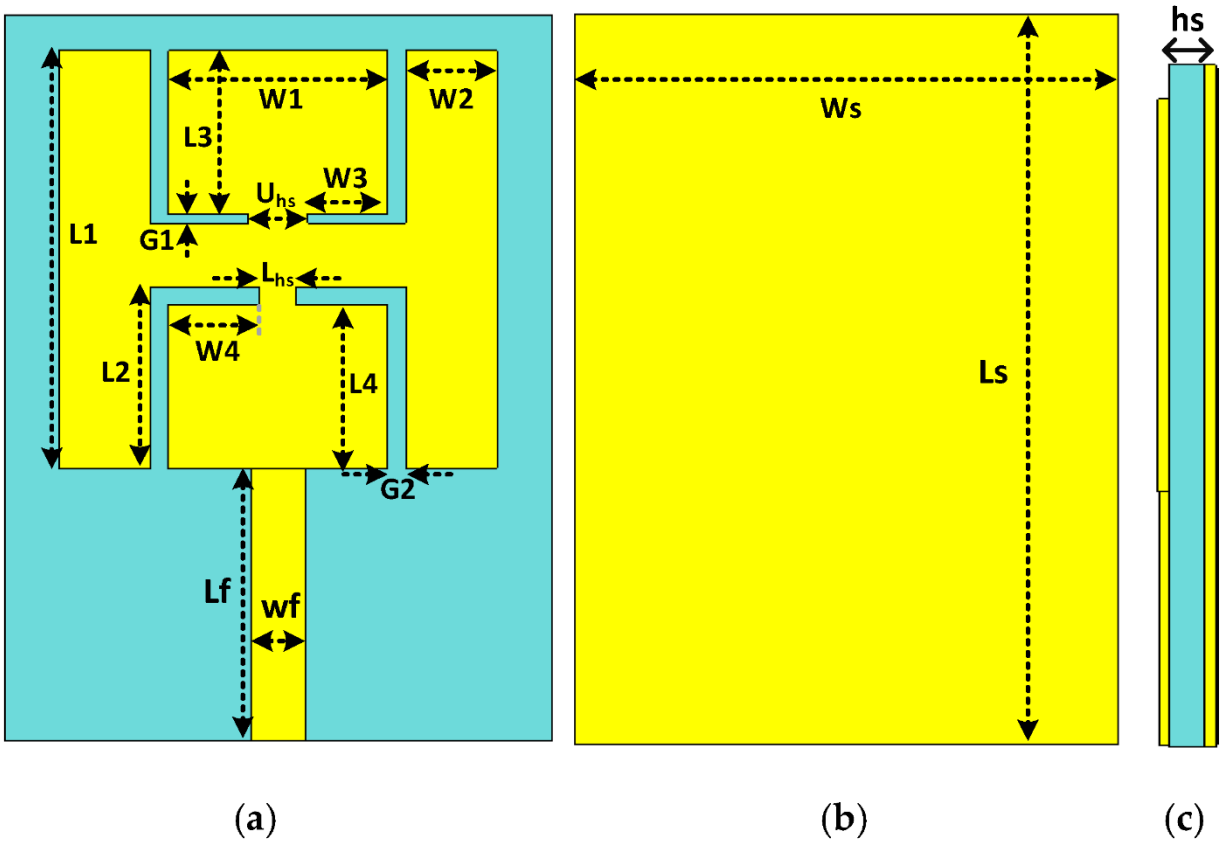

Figure 1 - (a) Patch Antenna layer (b) Ground layer (c) Substrate Thickness

- This based design was chosen for many characteristics cleared in those points :

  - **For Rectangular Patch:**
    - The rectangular patch is one of the simplest and most widely used shapes in microstrip antennas. Its straightforward geometry allows for easy analysis, fabrication, and integration with printed circuit boards (PCBs) & with optimizing the patch dimensions, a compact and efficient design can be achieved.

- **For Edge-Fed Configuration :**
  - The microstrip feed line at the edge can be easily optimized for impedance matching (≈ 50Ω) using established design techniques
  - Minimizes spurious radiation loss and ensures efficient power transfer to the patch.

- **For Slots in the Patch :**
  - The slot dimensions (length, width, and position) provide flexibility to adjust the resonant frequencies for specific applications
  - By altering the patch's effective length and creating multiple resonances, the slots can enhance the bandwidth.
  - Slots can help fine-tune the input impedance, improving the return loss (S11) and ensuring better impedance matching.
  - Slots introduce perturbations in the current distribution on the patch, creating additional resonant modes. This allows the antenna to operate at dual frequencies, making it ideal for multi-band applications.

- The patch antenna shown in **Figure 1** radiates in a dual-band because of the specific design features that alter the current distribution and resonant modes on the patch as follows :

  - **Resonance in a Microstrip Patch Antenna:**
    - A rectangular microstrip patch antenna operates by supporting standing wave modes. Its dominant mode is the TM_{10} mode, where the patch resonates when its effective length (L_{eff}) which is (L_1) to be approximately half the guided wavelength ($\lambda_{resonance}/2\sqrt{\varepsilon eff}$) of the operating frequency, The resonant frequency is expressed as:
    $F_{resonance} = \frac{c}{2L1\sqrt{\varepsilon eff}}$, where (εeff) is Effective permittivity of the substrate , (c) is the speed of light , $\lambda_{resonance} = c / F_{resonance}$

- When slots are introduced, the effective length of the patch is altered, supporting multiple resonant frequencies.

- **Effect of Slots on Dual-Band Radiation:**

  - The slots introduced into the patch significantly impact the current distribution and effective length of the patch
  - Enabling dual-band operation as the slots disrupt the uniform current flow across the patch
  - Increasing the current path length & introduces additional resonant modes since the effective length of the patch is extended locally by the slots
  - The specific dimensions and placement of the slots determine the resonant frequencies and the separation between the two bands
  -The higher frequency, the radiation pattern follows the typical broadside behaviour of a rectangular patch operating in the TM_{10} mode.
  - The lower resonance frequency Introduced by the slots, which add a new mode by locally increasing the effective length of the patch

- **Edge Feed and Excitation :**
  - The edge-fed configuration is optimized to excite both resonant modes effectively as the feed location is carefully chosen to match the impedance at both resonances ($\approx 50\Omega$).
  - The Matching ensures low return loss (S_{11}) and efficient radiation at both frequencies.

2.2 Measurements and Characterization of Design Scheme :

➢ The Design Scheme :

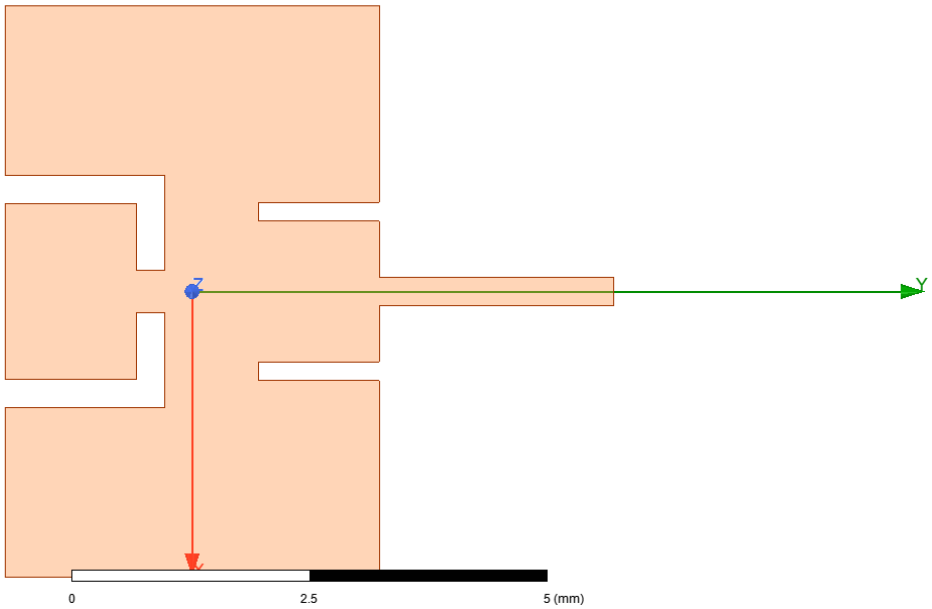

Figure 3 – Patch Design scheme Z-axis View

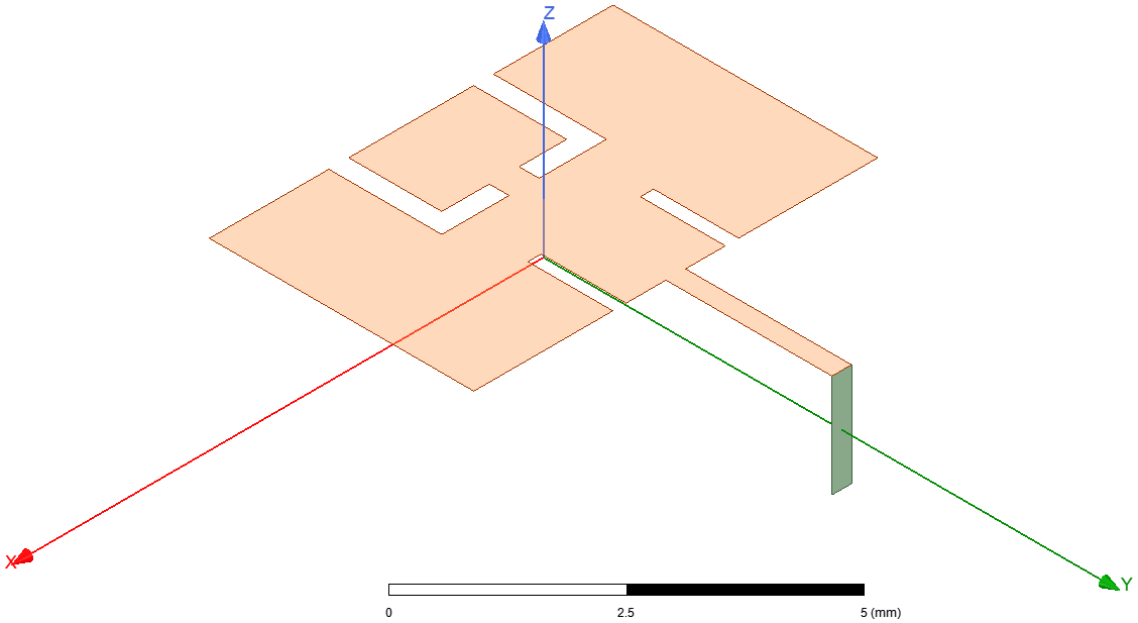

Figure 2 – Patch Design scheme Isometric View

- **Substrate Characterization :**

  - The choice of Substrate layer is FR4 substrate [4], with dielectric loss tangent 0.04 @30Ghz & 0.02 @15Ghz, relative permittivity 4.4 and height 1.6 mm is due to its good performance at high frequency as shown in Figure 1- (c)

- **Matching Networks Characterization :**

  - The Impedance of the single patch is ≈ 110 Ω

  - Each Patch should be matched with Quarter wave Section using characteristic impedance to be ≈ 110 Ω & with length $L_{QW} = \lambda_{resonance}/4\sqrt{\varepsilon eff}$ = 20 mm / 4 $\sqrt{4.4}$ = 2.38 mm & W_{QW} = 0.294 mm where $\lambda_{resonance} = 3x10^8 / 15x10^9 = 20$ mm

  - T-Section Network used to match the 2-element patches with characteristic impedance to be ≈ 110 Ω by Half Wave Section & with length $L_{HW} = \lambda_{resonance}/2\sqrt{\varepsilon eff}$ = 4.76 mm & W_{HW} = 0.5 mm

  - The main Feeding line is matched to make The Input Impedance to be ≈ 50 Ω , then the characteristic impedance to be ≈ 50 Ω By Half Wave Section with length $L_{feed} = \lambda_{resonance}/2\sqrt{\varepsilon eff}$ = 4.76 mm

- **Substrate & Patch Characterization [2] :**

Dimensions & Measurements formulas		
Dimension	**Measurement formula**	**Optimized Value**
$H_{substrate}$	$H_{substrate} \leq (0.3c / 2\pi F_{res}\sqrt{\varepsilon eff})$	**1.55 mm**
W_{patch}	$W_{patch} = \frac{c}{2f} * \sqrt{\frac{2}{\varepsilon r+1}}$	**6.08 mm**
ΔL ΔL is the extension length	$0.412\ H_{substrate} \frac{(\varepsilon eff+0.3)(\frac{Wpatch}{Hsubstrate}+0.264)}{(\varepsilon eff-0.258)(\frac{Wpatch}{Hsubstrate}+0.8)}$	**0.586 mm**
L_{patch}	$\frac{c}{2f\sqrt{\varepsilon eff}} - 2\,\Delta L$	**3.98 mm**
εeff	$\frac{\varepsilon r+1}{2} + \frac{\varepsilon r-1}{2} \frac{1}{\sqrt{1+12\frac{Hsubstrate}{Wpatch}}}$	**4.4**
$L_{sub} = L_{ground}$	$L_{patch} + 6\,H_{substrate}$	**21 mm**

$W_{sub} = W_{ground}$	$W_{patch} + 6\ H_{substrate}$	**14 mm**
W_1	$W_{slot} \approx 0.02\,\lambda_g$ to $0.1\,\lambda_g$, $\lambda_g = \lambda_o / \sqrt{\varepsilon eff}$	**0.94 mm**
W_3	$W_{slot} \approx 0.02\,\lambda_g$ to $0.1\,\lambda_g$	**0.5 mm**
W_4	$W_{slot} \approx 0.02\,\lambda_g$ to $0.1\,\lambda_g$	**0.5 mm**
L_2	$L_{slot} \approx 0.5\,\lambda_g$ to $0.25\,\lambda_g$, $\lambda_g = \lambda_o / \sqrt{\varepsilon eff}$	**1.32 mm**
L_3	$L_{slot} \approx 0.5\,\lambda_g$ to $0.25\,\lambda_g$, $\lambda_g = \lambda_o / \sqrt{\varepsilon eff}$	**1.02 mm**
L_4	$L_{slot} \approx 0.5\,\lambda_g$ to $0.25\,\lambda_g$, $\lambda_g = \lambda_o / \sqrt{\varepsilon eff}$	**1.02 mm**
U_{hs}	$U_{hs} \approx W_{patch} / 4$	**0.45 mm**
L_{hs}	$L_{hs} \approx L_{patch} / 4$	**0.94 mm**
G_1	$G_{slot} \approx 0.01\,\lambda_g$ to $0.05\,\lambda_g$, $\lambda_g = \lambda_o / \sqrt{\varepsilon eff}$	**0.3 mm**
G_2	$G_{slot} \approx 0.01\,\lambda_g$ to $0.05\,\lambda_g$, $\lambda_g = \lambda_o / \sqrt{\varepsilon eff}$	**0.3 mm**
W_{feed}	$W_{feed} = \frac{2Hsubstrate}{\pi} \{B - 1 - \ln(2B-1) + \frac{\varepsilon r - 1}{2\varepsilon r}[\ln(B-1) + 0.39 - (\frac{0.61}{\varepsilon r})]\}$ $B = \frac{377\pi}{2\,Zo\sqrt{\varepsilon r}}$	**3.5 mm**

2.3 Design Specification:

- **Return Loss :**

  - It is recommended that the Return Loss **(S_{11})** at the resonance frequency due to matching to be **less than -10dB**

- **Input Impedance :**

- - It is recommended that the input impedance **(Z_{11})** at the resonance frequency due to matching to be ≈ **50 ohm & Reflection Coefficient Less than 0.2**

- **Peak Gain :**

  - It is recommended that the Peak Gain at the resonance frequency in the boresight to be **more than 2dB**

- **Radiation Efficiency :**

  - It is recommended that the Radiation Efficiency at the resonance frequency due to low ohmic power loss to be **more than 70%**

- **XPD (Cross-Polar Discrimination) :**

  - It is recommended that the XPD at the resonance frequency due to linear polarization to be **less than -10dB** as it is polarized in the **Phi direction**

- **VSWR (Voltage Standing Wave Ration) :**

  - It is recommended that the VSWR at the resonance frequency due to matching to be **less than 2**

- **Front to Back Ratio :**

  - It is recommended that the Front to Back Ration at the resonance frequency due to Directivity to be **more than 10**

3. Result & Discussion :

3.1 Verification of EM tool [3] :

- To validate the functionality of the HFSS electromagnetic tool, we aim to construct an **inset fed patch antenna**. This involves computing the radiation impedance and analysing the radiation pattern, anticipating that it aligns closely with the theoretical predictions.

- The intention of the patch antenna to operate at **2.4GHz**

3.1.1 Design:

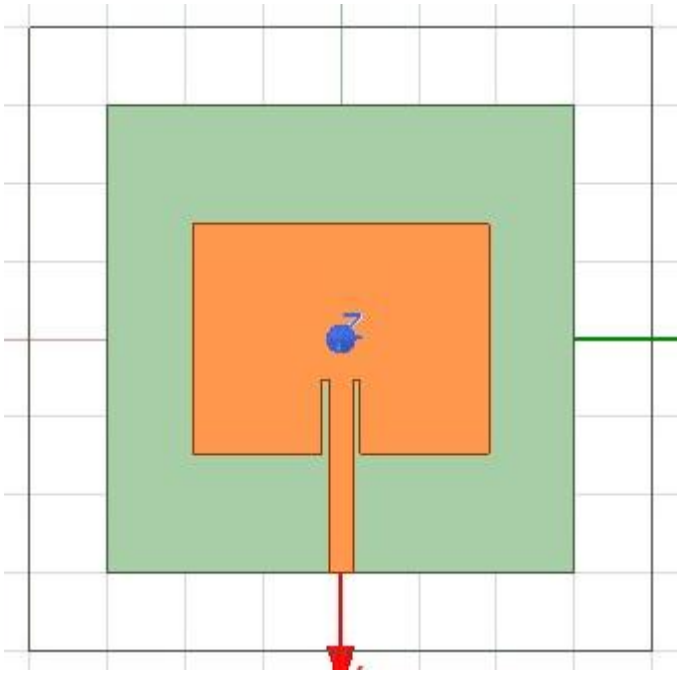

Figure 4 - Patch Antenna Z-axis View

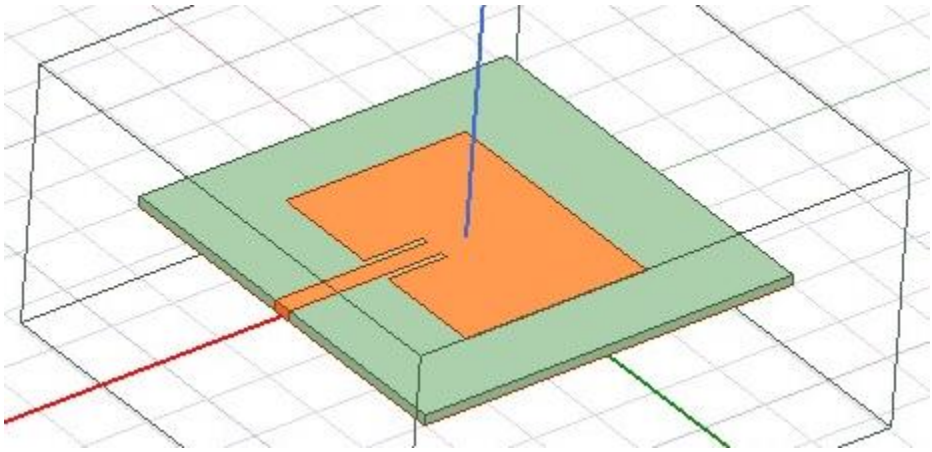

Figure 5- Patch Antenna Isometric View

3.1.2 Results:

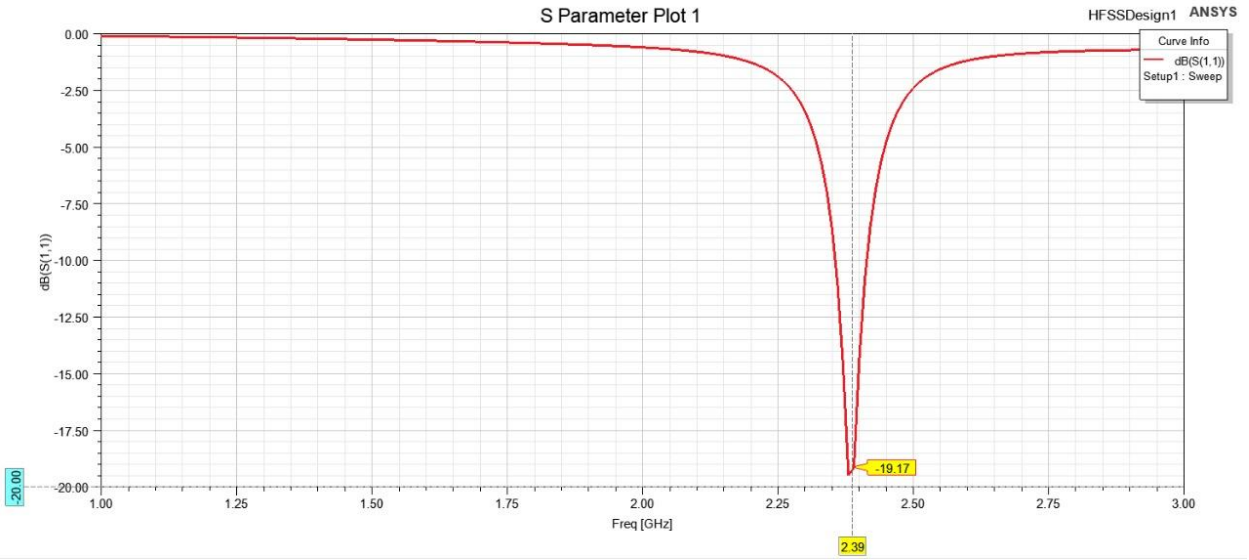

Figure 6 - Return loss (S11) of Patch Antenna

- The **Return Loss** is **-19.17dB** in the resonance frequency 2.4GHz Which indicating a perfect matching in the operating frequency

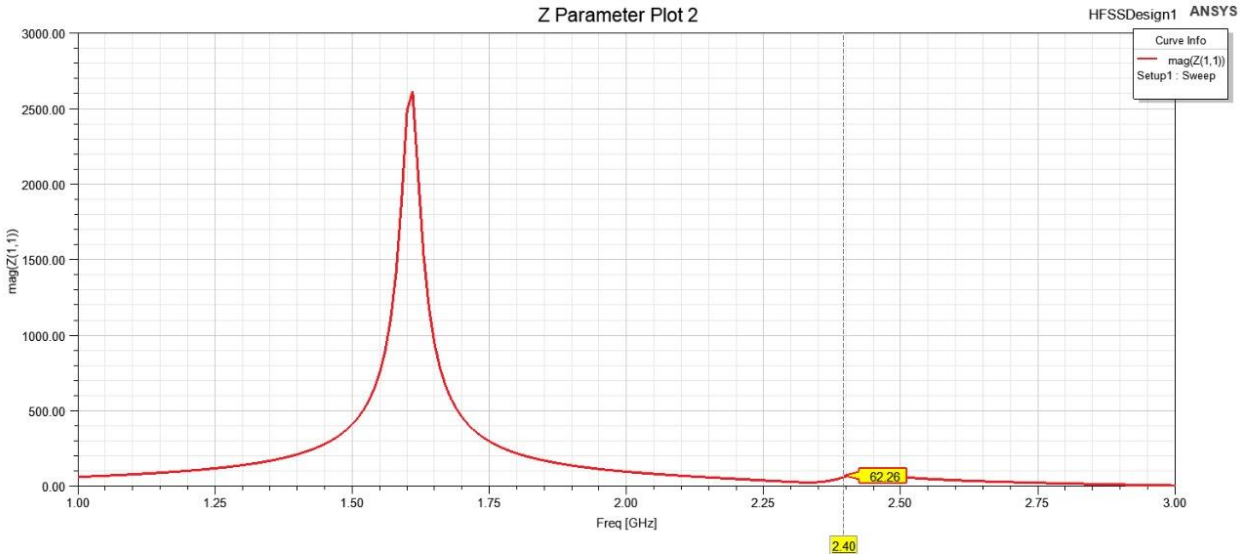

Figure 7 - Input Impedance of Patch Antenna

- The **Input Impedance** is **62.26 Ω** at the resonance frequency which is matched with source port impedance ≈ 50 Ω

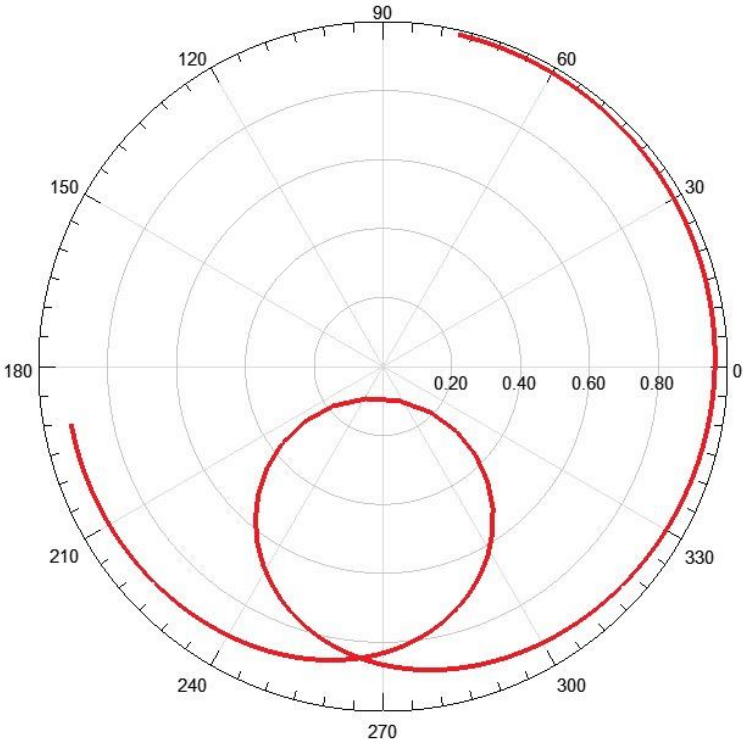

Figure 8 - Input Impedance of Patch Antenna in Smith Chart

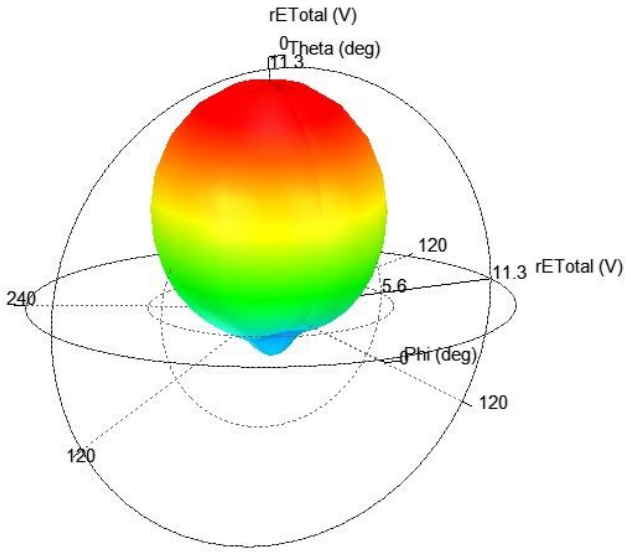

Figure 9 - 3D Radiation Pattern Gain of Patch Antenna

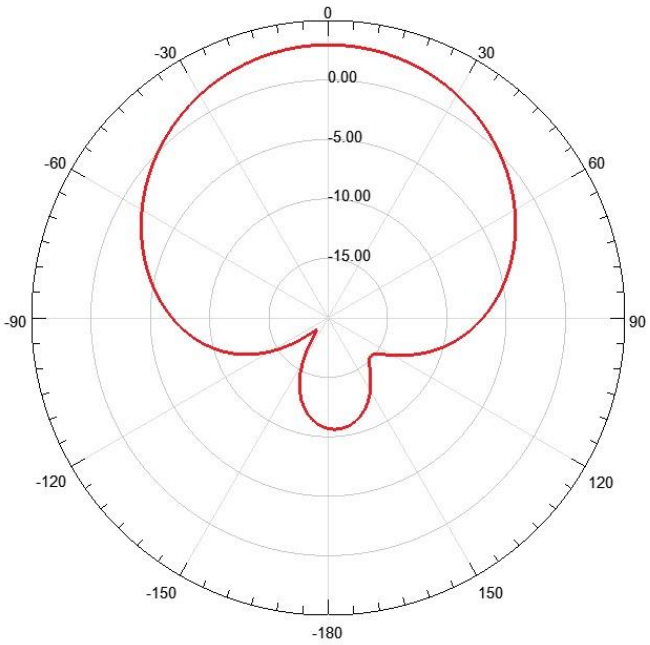

Figure 10 - E Plane Radiation Pattern

- The **Peak Gain in E-Plane** is **3.7 dB** in the resonance frequency **2.4GHz** at **Phi = 0**

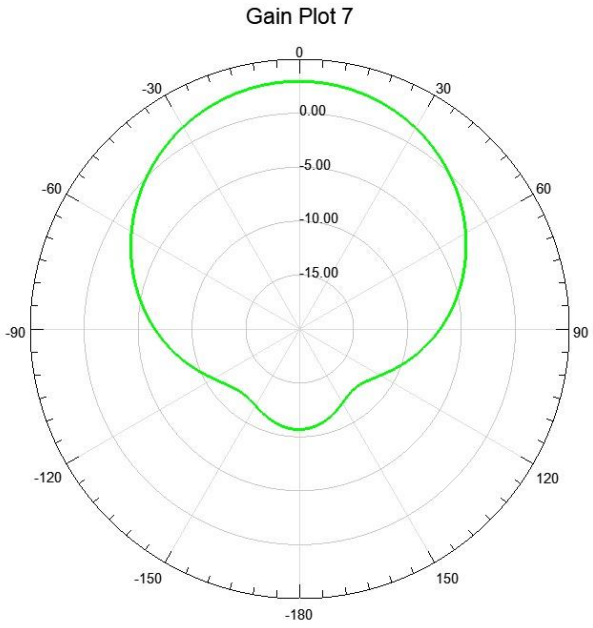

Figure 11 - H Plane Radiation Plane of Patch Antenna

- The **Peak Gain in H-Plane** is **3.7 dB** in the resonance frequency **2.4GHz** at **Phi = π / 2**

3.1.3 Conclusion:

- The successful alignment of the designed patch antenna with the theoretical values indicates the completion of the verification phase. This achievement demonstrates the accurate functionality and proper execution of HFSS, affirming its reliability in accurately modelling and predicting antenna performance.

3.2 Simulations and Analysis:

- Design Scheme of The Single Patch Antenna:

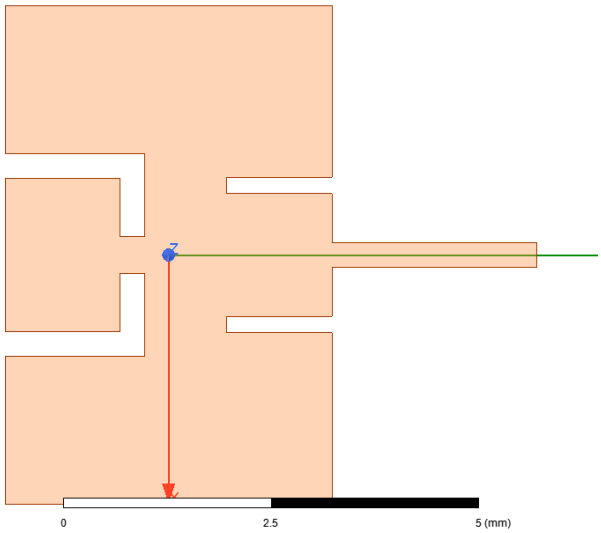

Figure 12 - Design Scheme of The Single Patch Antenna Z-axis View

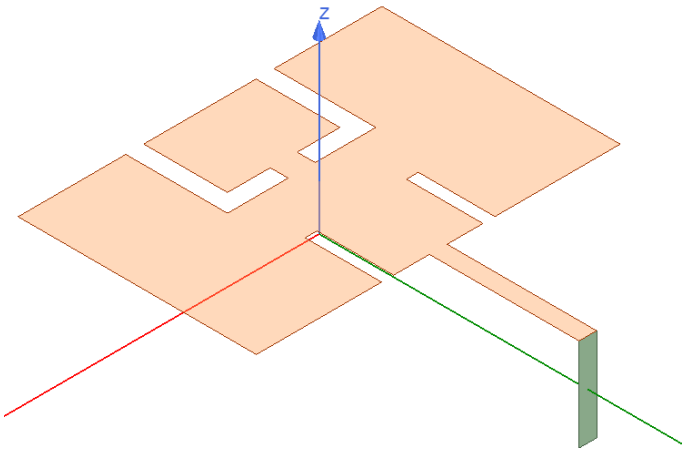

Figure 13 - Design Scheme of The Single Patch Antenna Isometric View

- **Return Loss of The Single Patch Antenna (S_{11}):**

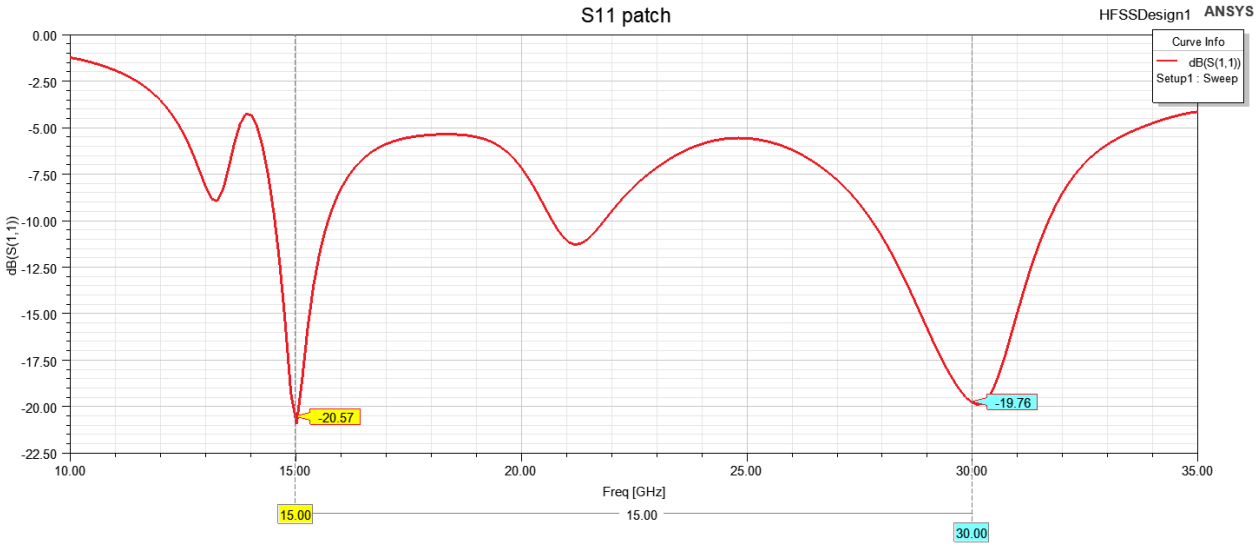

Figure 14 - Return Loss (S11) of The Single Patch Antenna

- Achieving a Return loss of **-20.57dB at 15 GHz** & **-19.76 dB at 30 GHz** , signifies robust impedance matching and operational versatility, ensuring minimal signal reflections and a wide operational frequency range for diverse communication applications, shown in Figure 14.

3.2.1 Return Loss (S_{11}):

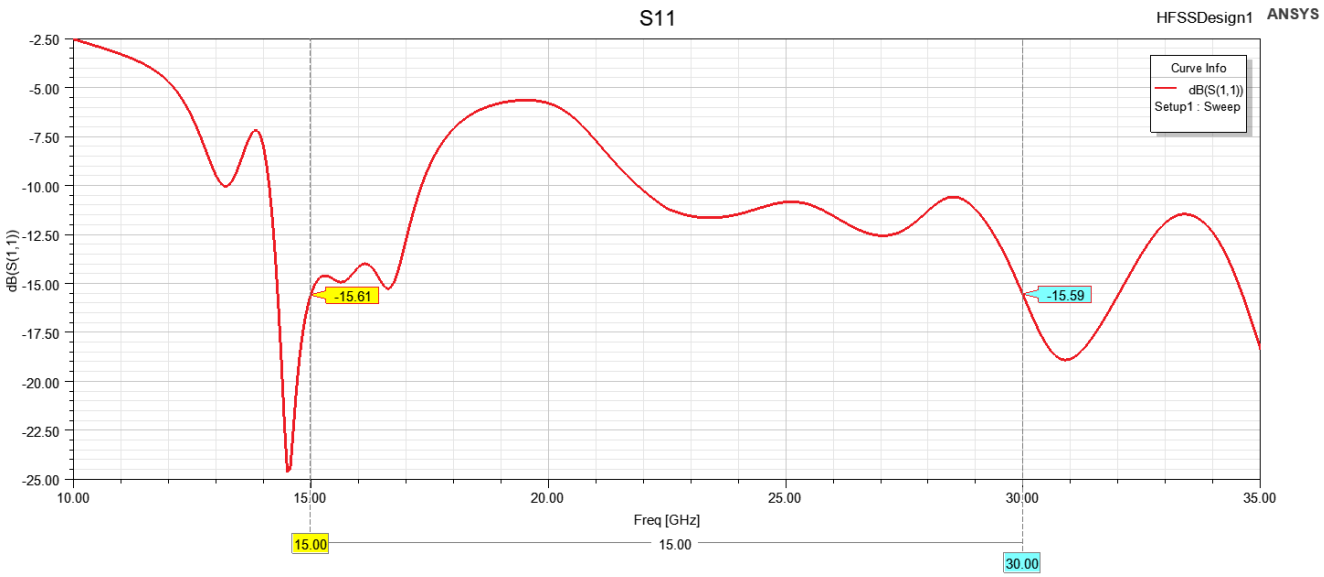

Figure 15 - Return Loss (S11)

- Achieving a **Return loss** of **-15.61dB at 15 GHz** & **-15.59dB at 30 GHz** , also meeting the design specifications mentioned to be get a Return Loss less than -10dB at the both operating frequencies , Signifies robust impedance matching and operational versatility and significant resonance at the both frequencies, ensuring minimal reflections and a wide operational frequency range for diverse applications, shown in Figure 15.

3.2.2 Input Impedance (Z_{11}):

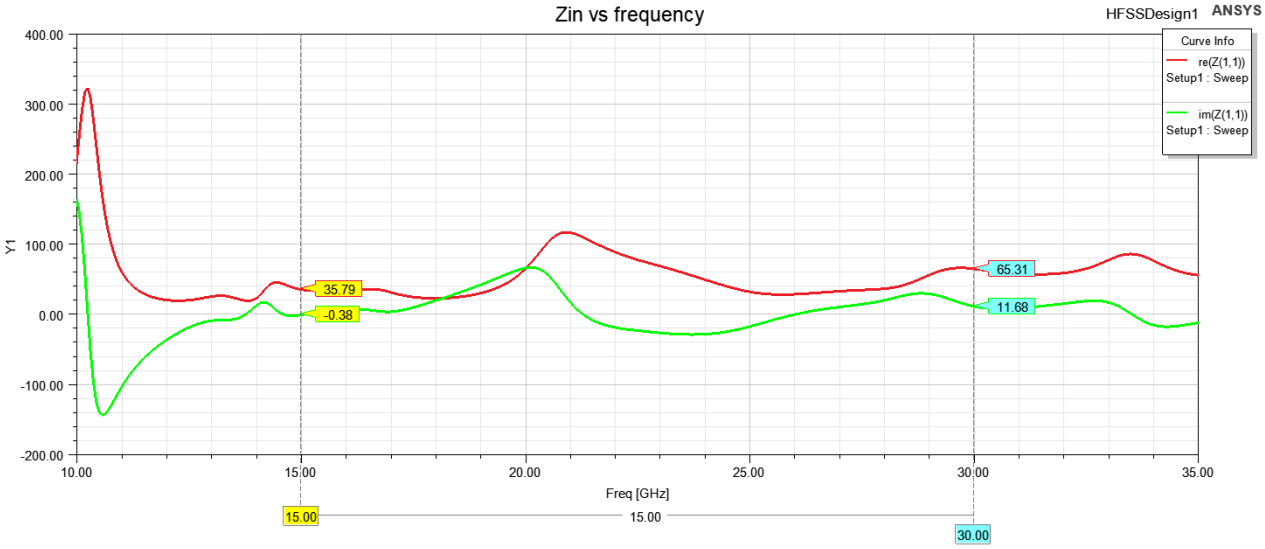

Figure 17 - Input Impedance (Z11)

Name	Freq	Ang	Mag	RX
m1	15.0000	-0.6808	35.7482	-1.0576 - 0.0007i
m2	30.0000	10.1823	66.2996	-1.0301 + 0.0055i

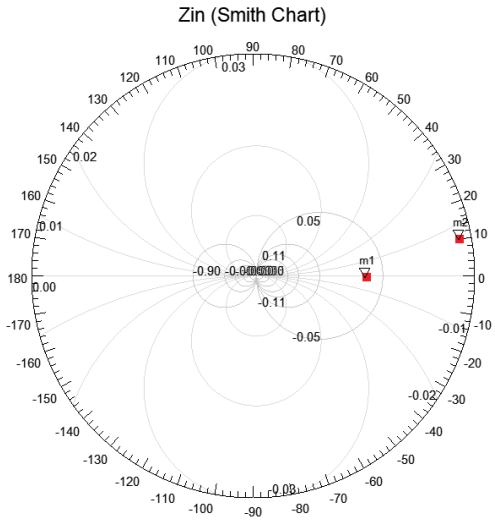

Figure 16 - Input Impedance on Smith Chart

- Attaining an **input impedance** of **35.79Ω at 15 GHz** & **65.31Ω at 30 GHz** signifies high matching, aligning seamlessly with standard requirements for optimal power transfer and signal integrity within the specified frequency range, Also meeting the design specifications mentioned to be get Input Impedance near 50 Ω at the both operating frequencies & **to get Reflection Coefficient Less than 0.2**

3.2.3 The Radiation Pattern (Co-Pol & X-Pol) in E & H Planes:

Name	Theta	Ang	Mag
m1	0.0000	0.0000	5.8516
m2	0.0000	0.0000	-34.2723

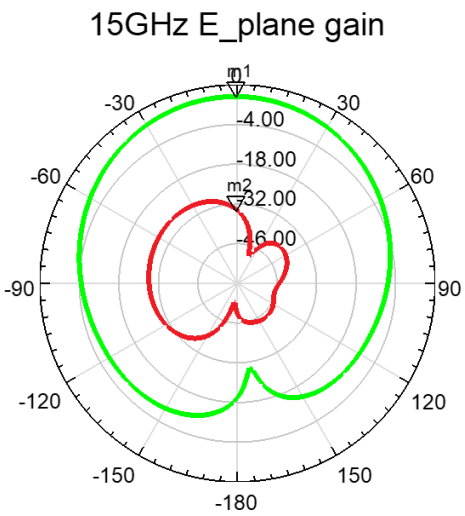

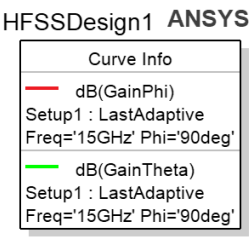

Figure 18 - E Plane Radiation Pattern @15GHz

- The **E-plane Gain** plot at **15 GHz** shows the **co-polarized gain (GainTheta)** achieving a maximum of **5.85 dB**, while the **X-polarized gain (GainPhi)** is significantly lower at **-34.27 dB**. This results in a high cross-polarization discrimination **(XPD) of approximately 40 dB**, indicating excellent polarization purity. The antenna demonstrates strong directional performance with minimal interference from unwanted polarization, making it suitable for applications requiring high polarization selectivity.

- The alignment of the feed line parallel to the **Y-axis** resulted in current flow along the **Y-direction**, positioning the **E-plane within the YZ plane at a Phi of 90 degrees.**

- The alignment of the feed line parallel to the **Y-axis** resulted in current flow along the **Y-direction**, positioning the **H-plane within the XZ plane at a Phi of 0 degrees**.

Name	Theta	Ang	Mag
m1	0.0000	0.0000	5.8516
m2	0.0000	0.0000	-34.2723

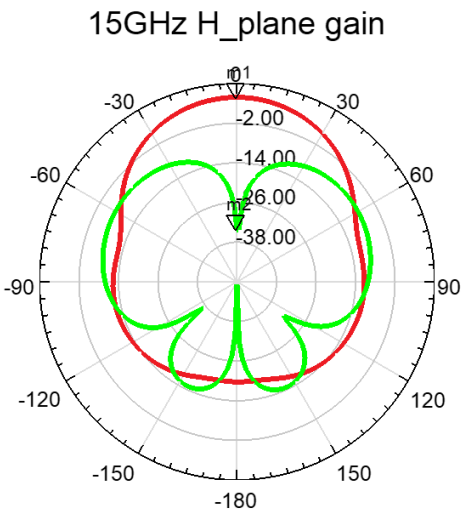

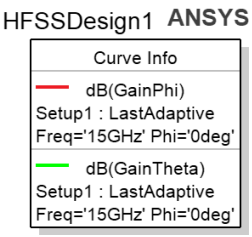

Figure 19 - H Plane Radiation Pattern @15GHz

- The **H-plane Gain** plot at **15 GHz** illustrates the **co-polarized gain (GainPhi)** reaching a maximum of **5.85 dB**, while the **X-polarized gain (GainTheta)** is significantly lower at **-34.27 dB**. This results in a cross-polarization discrimination **(XPD) of approximately 40 dB**, highlighting excellent polarization isolation. The antenna exhibits strong directional radiation in the H-plane with minimal interference from unwanted polarization. This performance is suitable for applications requiring high polarization purity and controlled beam patterns.

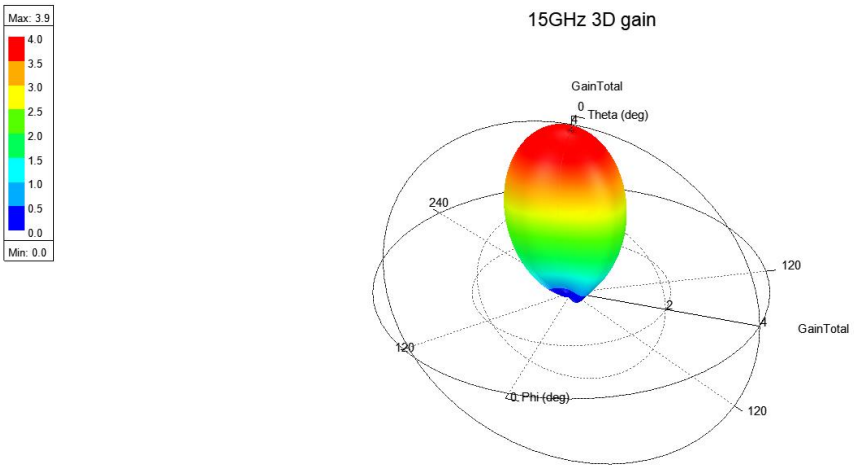

Figure 20 - 3D Gain Radiation Pattern @ 15 GHz

- The **3D Gain** plot at **15 GHz** shows a **strong directional radiation pattern** with a maximum gain of approximately **3.9 dBi**, indicating efficient energy concentration in a specific direction.

Name	Theta	Ang	Mag
m1	0.0000	0.0000	7.4413
m2	0.0000	0.0000	-30.8218

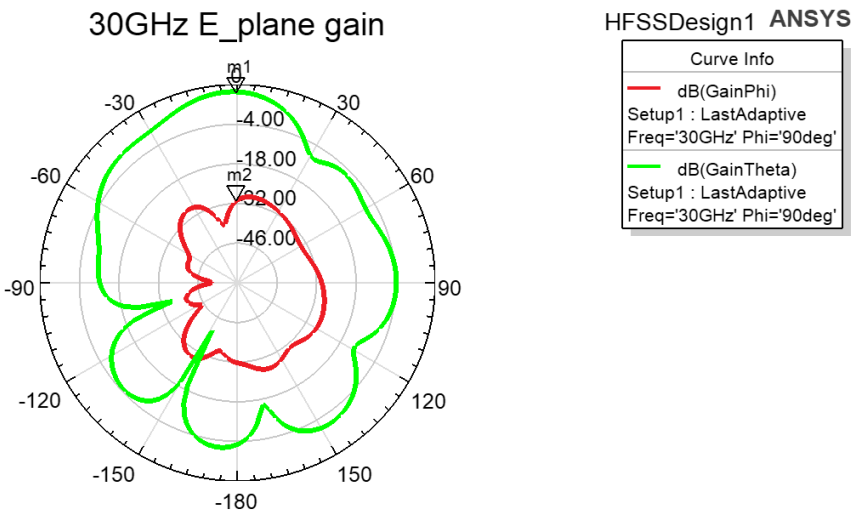

Figure 21 - E Plane Radiation Pattern @ 30GHz

- The **E-plane Gain** plot at **30 GHz** shows the **co-polarized gain (GainTheta)** achieving a maximum of **7.44 dB**, while the **X-polarized gain (GainPhi)** is significantly lower at **-30.82 dB**. This results in a high cross-polarization discrimination **(XPD) of approximately 38.26dB**, indicating excellent polarization purity. The antenna demonstrates strong directional performance with minimal interference from unwanted polarization, making it suitable for applications requiring high polarization selectivity.

Name	Theta	Ang	Mag
m1	0.0000	0.0000	7.4413
m2	0.0000	0.0000	-30.8218

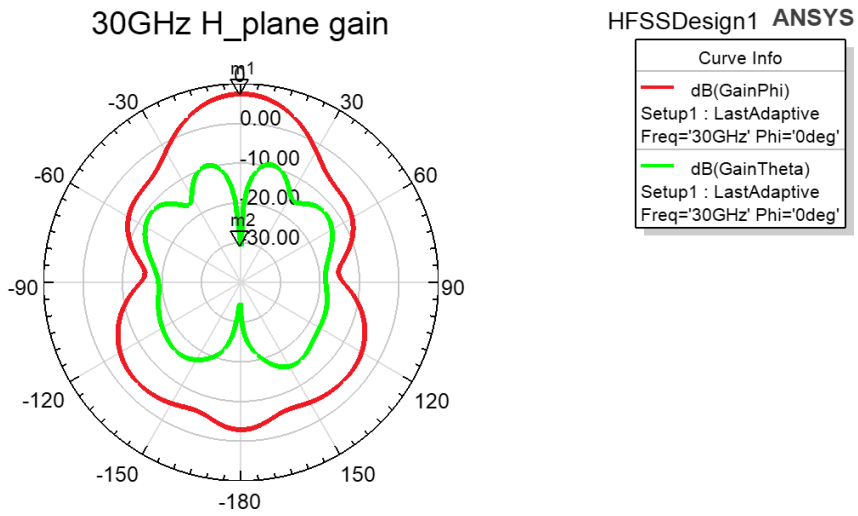

Figure 22 - H Plane Radiation Pattern @ 30GHz

- The **H-plane Gain** plot at **30 GHz** illustrates the **co-polarized gain (GainPhi)** reaching a maximum of **7.44 dB**, while the **X-polarized gain (GainTheta)** is significantly lower at **-30.82 dB**. This results in a cross-polarization discrimination **(XPD) of approximately 37.26 dB**, highlighting excellent polarization isolation. The antenna exhibits strong directional radiation in the H-plane with minimal interference from unwanted polarization. This performance is suitable for applications requiring high polarization purity and controlled beam patterns.

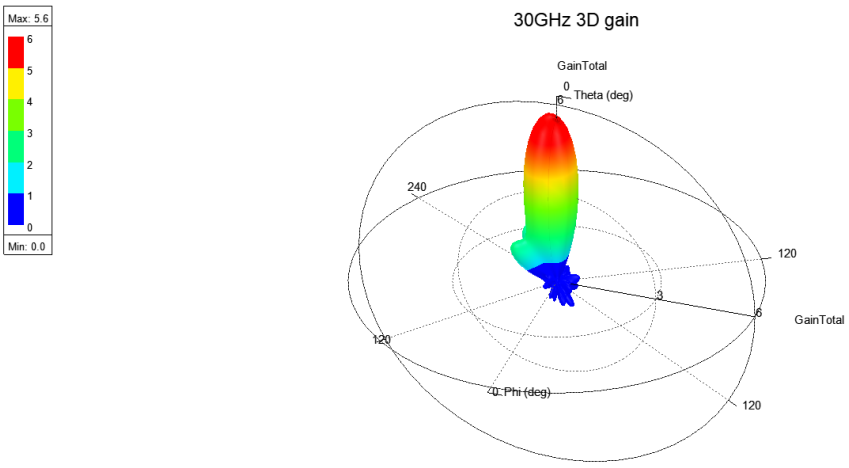

Figure 23 - 3D Gain Radiation Pattern @ 30 GHz

- The **3D Gain** plot at **30 GHz** shows a **highly directional radiation pattern** with a maximum gain of approximately **5.6 dBi**, indicating efficient energy concentration in a specific direction.

3.2.4 The Peak Gain:

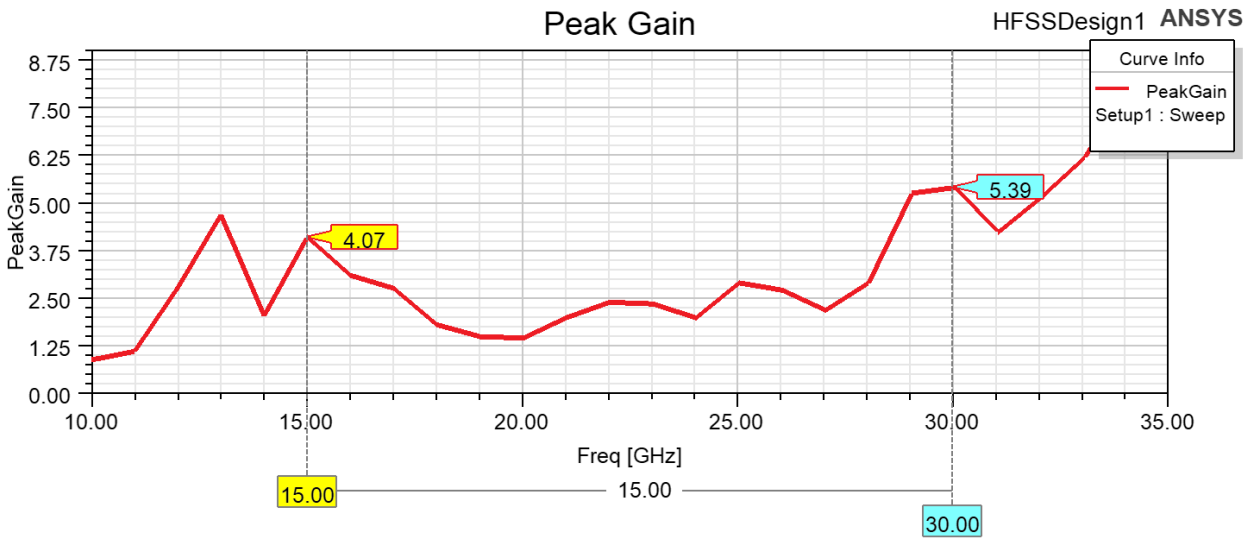

Figure 24 - Peak Gain

- The **Peak Gain** plot illustrates the antenna's performance across a range of frequencies. The gain exhibits a varying characteristic, reaching a maximum value of **5.39 at approximately 30 GHz**. Another notable peak of **4.07 is observed around 15 GHz**. This behavior highlights the frequency-dependent nature of the antenna's gain, with certain frequency bands demonstrating superior performance compared to others.

3.2.4 The Radiation Efficiency:

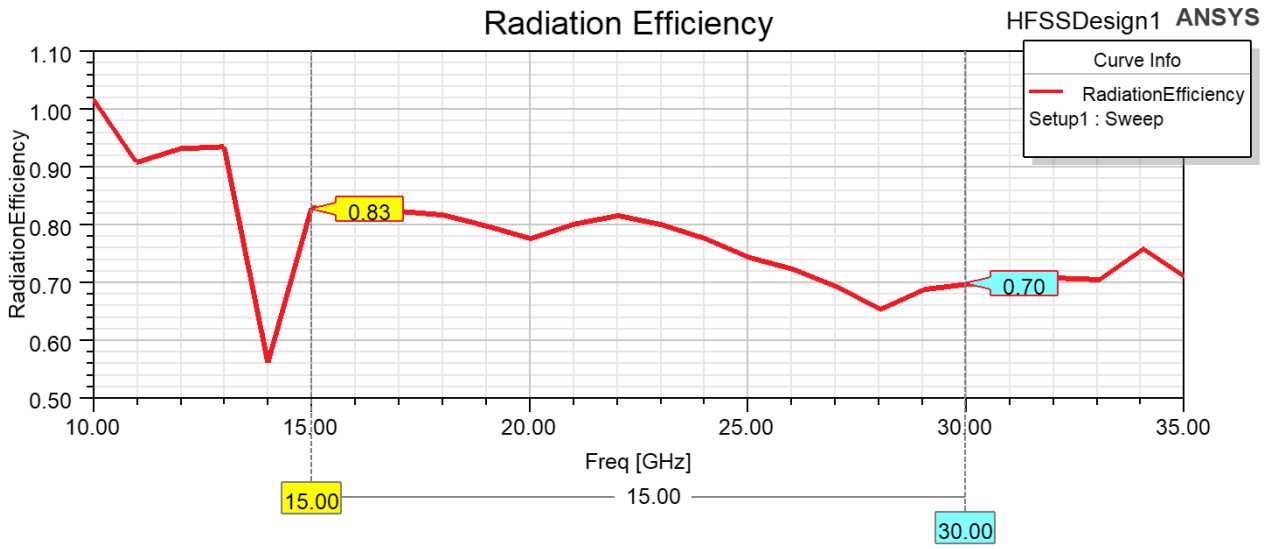

Figure 25 - Radiation Efficiency

- The **Radiation Efficiency** plot illustrates the antenna's efficiency across a range of frequencies. The efficiency exhibits a varying characteristic, reaching a maximum value of **0.83 at approximately 15 GHz**. A minimum efficiency of **0.70 is observed around 30 GHz**. This indicates that the antenna's performance is frequency-dependent, with certain frequency bands demonstrating higher efficiency than others, And Also meeting the design specifications mentioned to be get **Radiation Efficiency more than 70%**

3.2.5 More Characteristics:

- **XPD :**

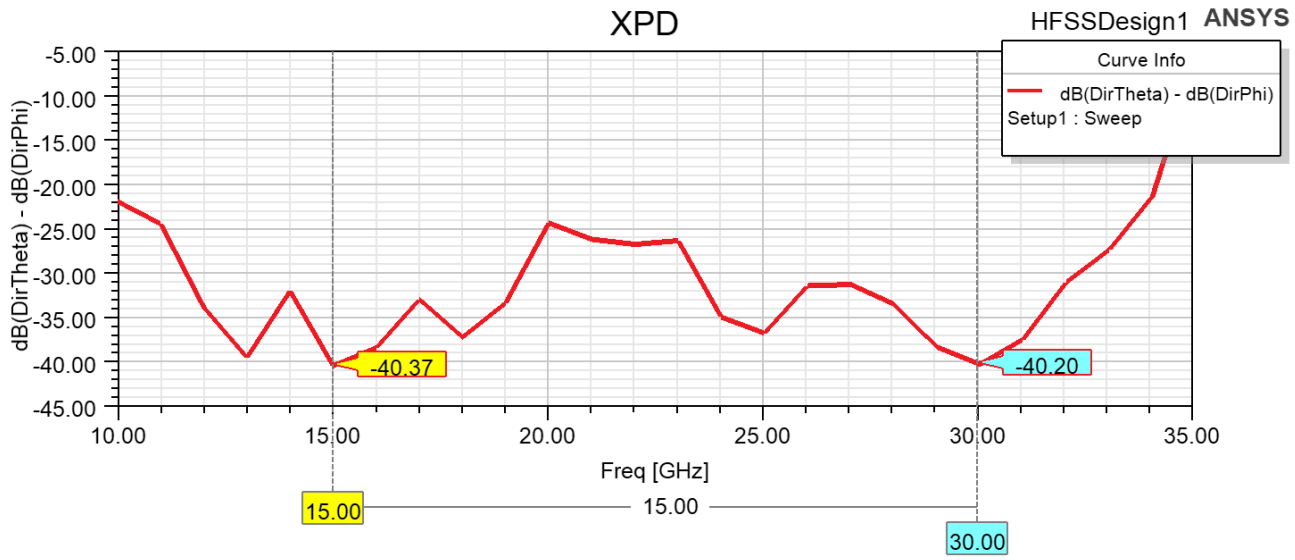

Figure 26 - XPD

- The **XPD** plot, which represents the difference between the **co-polarized gain (in Theta direction)** and the **cross-polarized gain (in Phi direction)**, shows a varying characteristic across the frequency range. **XPD** reaches a maximum value of **-40.20 dB** at **30 GHz** and a minimum value of **-40.37 dB at 15 GHz**. This indicates that the antenna's performance in terms of suppressing polarization in the **Phi direction** is frequency-dependent.This explicitly states that the **XPD** plot measures the suppression of **polarization in the Phi direction.**

➢ Front-to-Back Ratio (FBR):

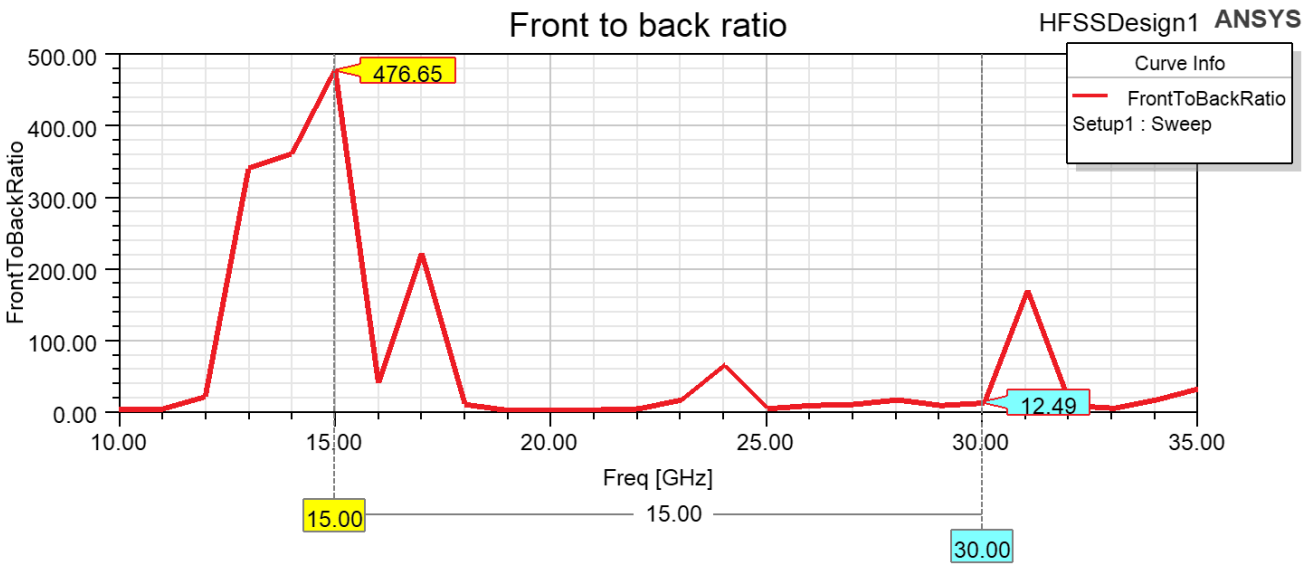

Figure 27 - Front-To-Back Ratio (FBR)

- The **Front-to-Back Ratio (FBR)** plot illustrates the antenna's ability to direct radiation forward while minimizing radiation in the backward direction. The FBR exhibits a varying characteristic across the frequency range, reaching a maximum value of **476.65 at approximately 15 GHz**. A minimum ratio of **12.49 is observed around 30 GHz**. This indicates that the antenna's performance in terms of suppressing backward radiation is frequency-dependent, with certain frequency bands demonstrating significantly better front-to-back performance than others & meeting the design specifications mentioned to **get high FBR**

➢ Voltage Standing Wave Ratio (VSWR) :

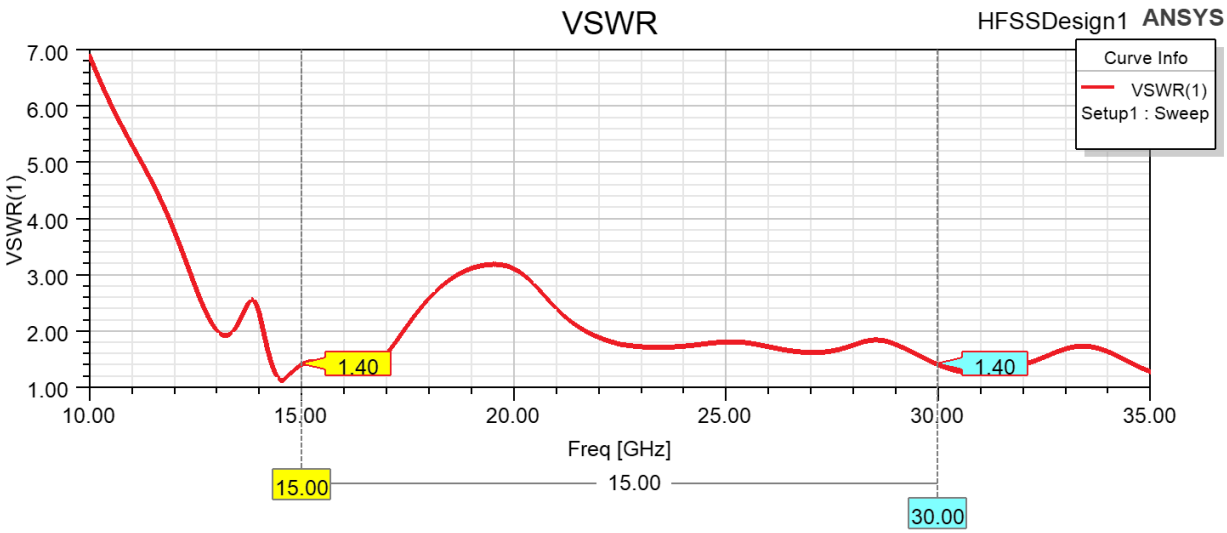

Figure 28 - Voltage Standing Wave Ratio (VSWR)

- The **VSWR (Voltage Standing Wave Ratio)** plot shows the variation of VSWR across the frequency range. VSWR measures the impedance mismatch between the antenna and the transmission line. Ideally, **VSWR should be close to 1.0**, indicating a good impedance match. In this case, the VSWR exhibits a varying characteristic, reaching a minimum value of **1.40 at both around 15 GHz and 30 GHz**. At these frequencies, the antenna exhibits a better impedance match with the transmission line, resulting in lower losses and improved power transfer. However, the VSWR rises significantly at other frequencies, indicating higher impedance mismatch and potentially increased losses.

➢ Mutual Coupling Between The Antenna 2-Elements :

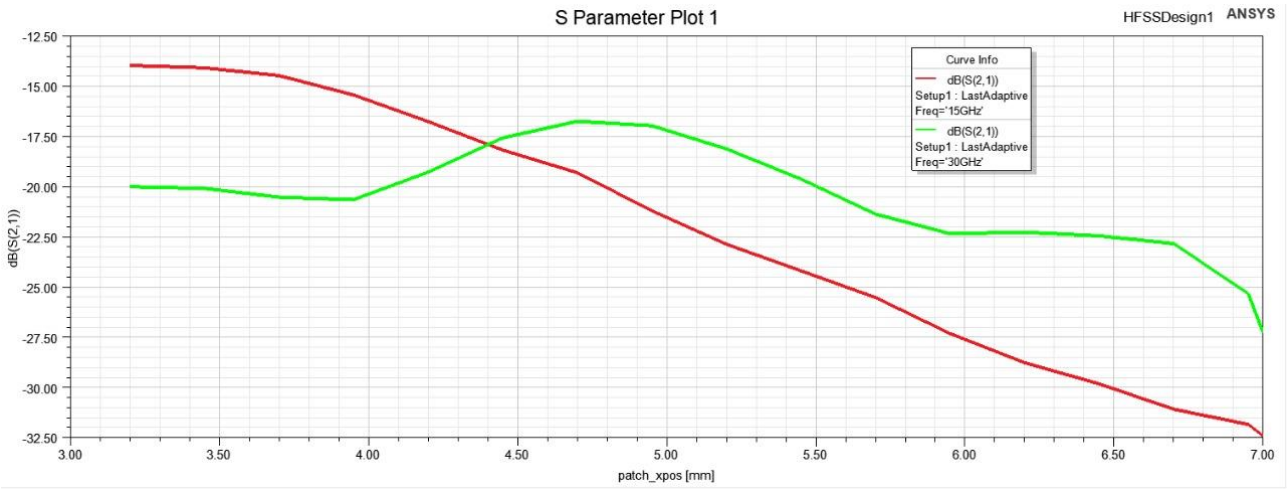

Figure 29 - Mutual Coupling vs Element spacing @ 15GHZ & 30 GHz

- The S_{21} plot reveals the **mutual coupling** between the two elements of the antenna array at 15GHz & 30GHz versus the element spacing (**patch_xpos**).
- The S_{21} parameter, representing the transmission coefficient from one element to the other, indicates the level of coupling. Higher S21 values suggest stronger coupling, while lower values indicate weaker coupling.
- The plot also shows how this coupling at **15GHz & 30GHz** varies with position (**patch_xpos**), which is crucial for understanding the array's performance and optimizing its design.

- The chosen separation is **4.5 mm** for S_{21} to be **-17.5 dB @ 30 Ghz** & **-18 dB @ 15 GHz**

3.2.6 Equivalent circuit model:

- **Circuit Parameters Variables:**

Figure 30 - Circuit Parameter Variables

- **Equivalent Circuit Model:**

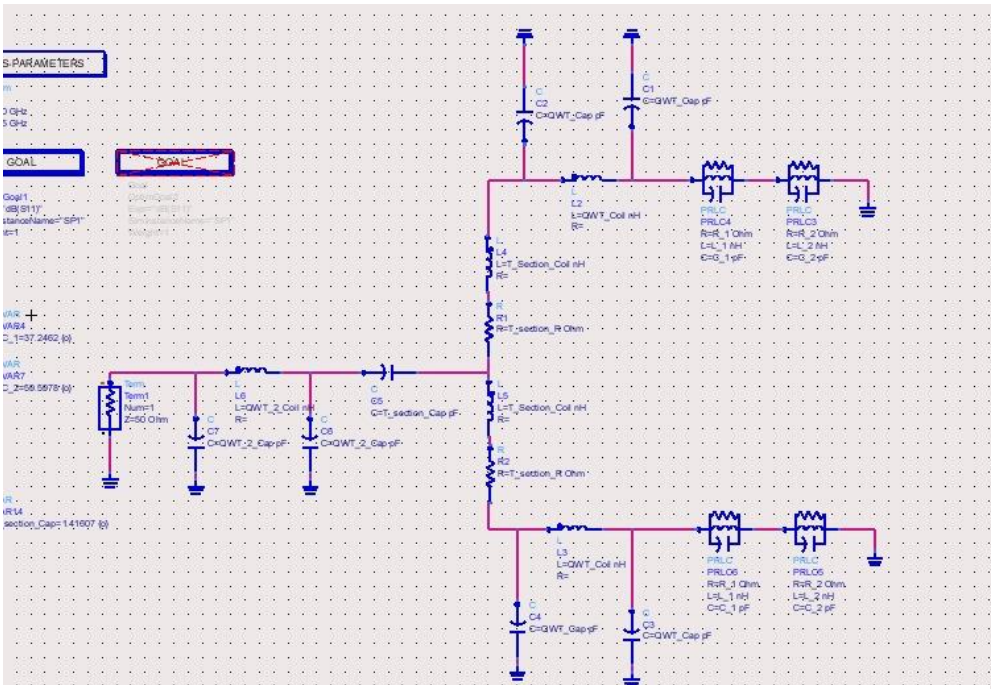

Figure 31 - Equivalent Circuit Model

- **Equivalent Circuit Model labeling:**

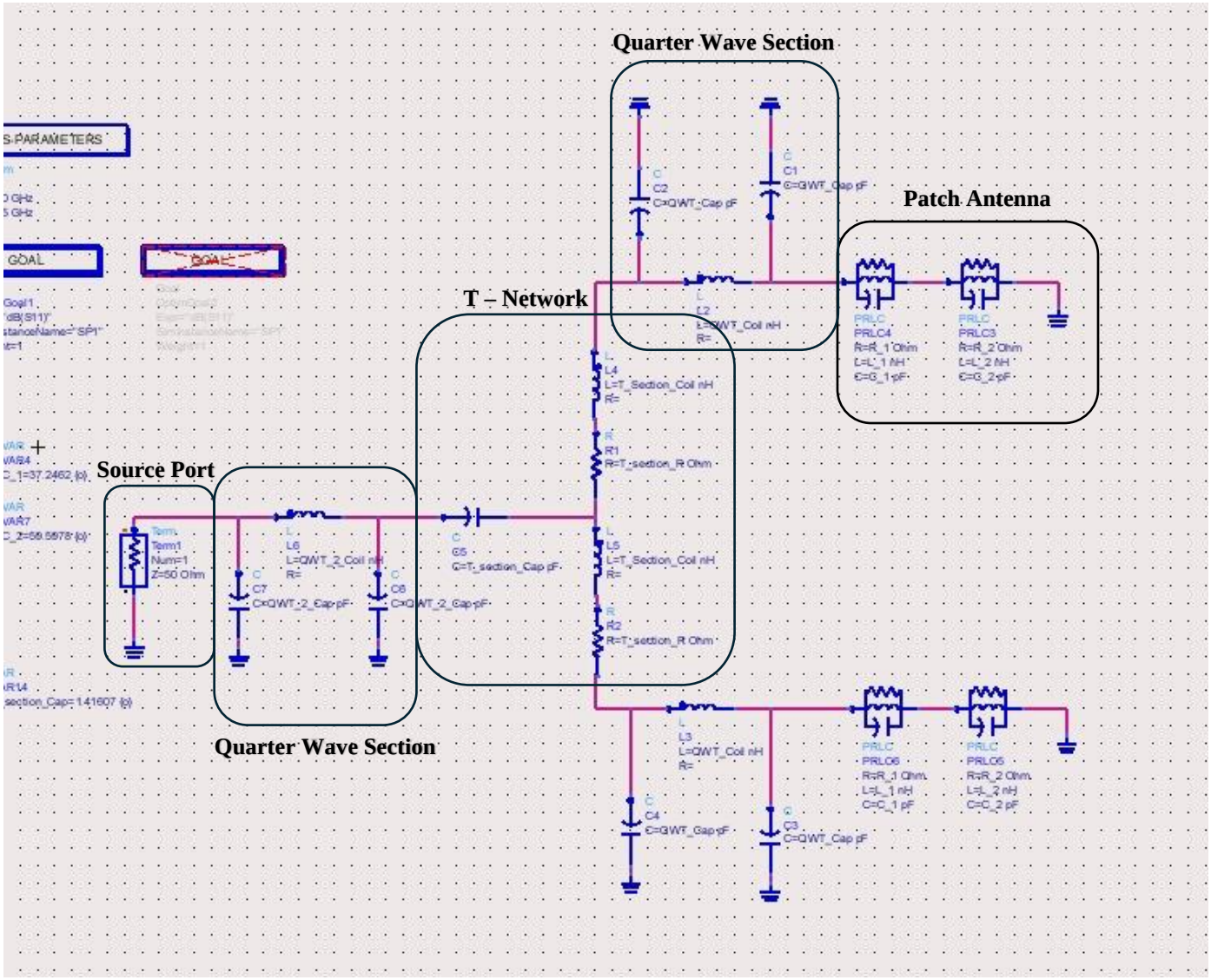

Figure 32 - Equivalent Circuit Model Labeling

- **Equivalent Circuit Return Loss (S_{11}):**

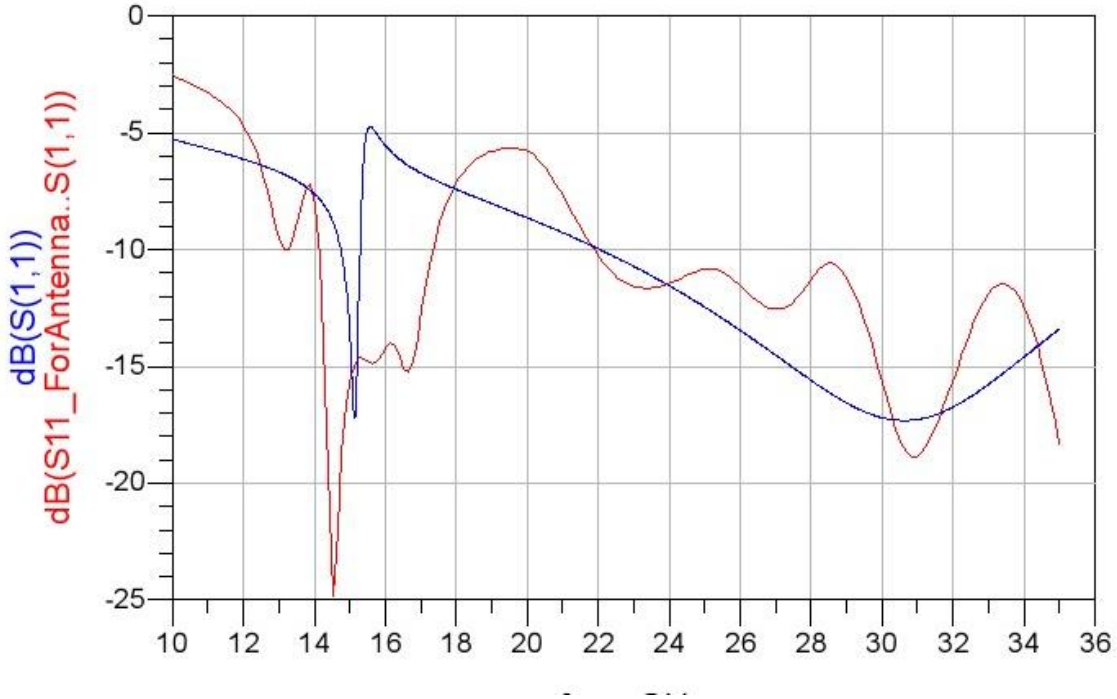

Figure 33 - Equivalent Circuit Return Loss (S11)

- The resulting Return Loss is the same Return Loss got by The EM Tool in the plot of the S_{11} which reach **-15.61dB at 15 GHz** & **-15.59dB at 30 GHz ,** which indicates that the circuit model has high accuracy for performing the function of the Antenna design.

4. Final Design Layout:

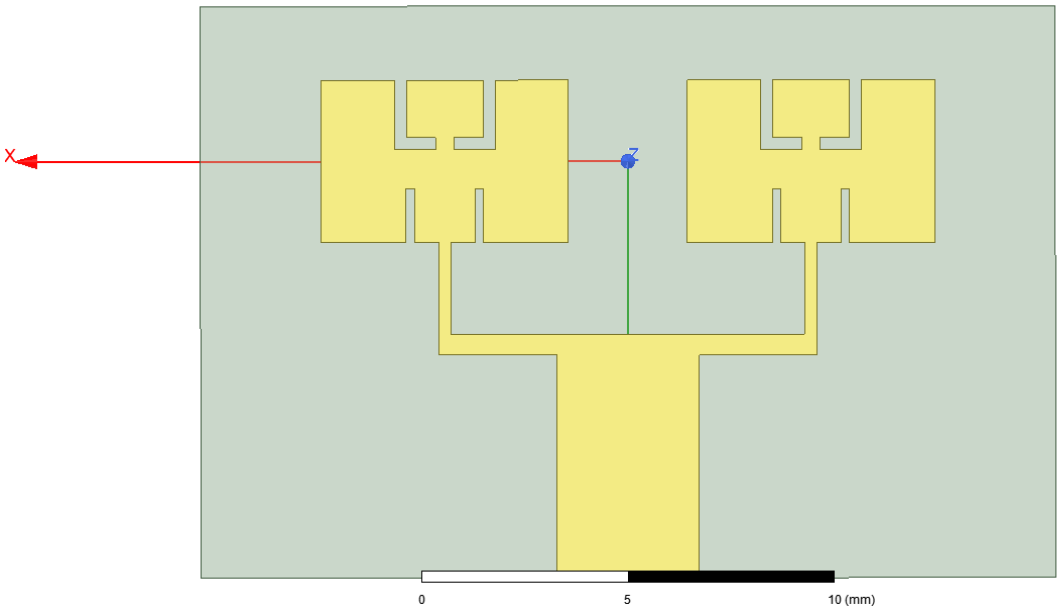

Figure 34 - Final Design Layout Z-axis View

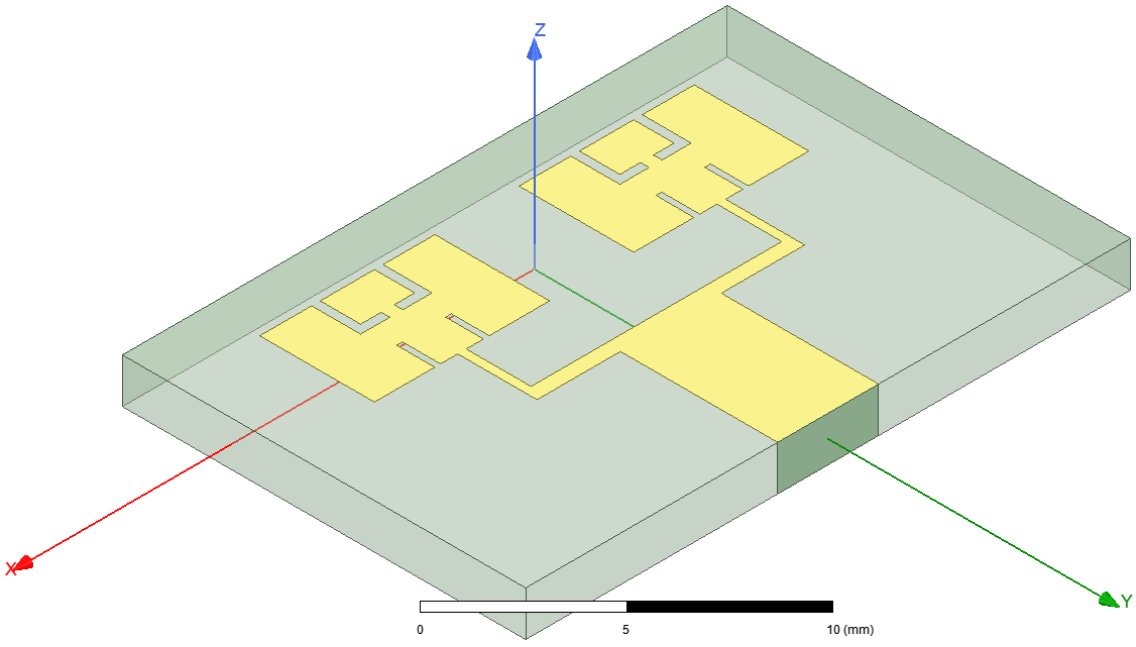

Figure 35 - Final Design layout Isometric Layout

- That **Final Design layout Antenna Design** appears to be a planar, microstrip patch antenna with multiple feed lines. The complex geometry with multiple radiating elements and feed structures suggests a deliberate approach to achieving dual-band operation at **15 GHz** and **30 GHz.** The design likely incorporates techniques such as parasitic elements, notches, or slots to introduce resonances at the desired frequencies. The multiple feed lines may be used to control the excitation of the different resonant modes and optimize the antenna's radiation pattern and impedance matching at both operating frequencies.

5. Conclusion:

- In conclusion, this exhaustive exploration and meticulous design journey have yielded an exemplary edge-fed dual band 2-element antenna system, resonating at 15GHz & 30GHz with impeccable precision. Through an intricate balance of theory and practical implementation, we've achieved not just a design, but an embodiment of engineering excellence. This antenna showcases not only superior performance in terms of return loss, bandwidth, and radiation characteristics but also embodies the culmination of relentless refinement and innovation. Its success underscores not just a technical feat, but a testament to the pursuit of pushing boundaries, setting a benchmark for future advancements in high-frequency antenna engineering.

6. References:

[1] **Compact Dual-Band Antenna with Paired L-Shape Slots for On- and Off-Body Wireless Communication**

[2] **Design and simulation of dual-band rectangular microstrip patch array antenna for millimeter-wave**

[3] **Design of 2.4GHz Patch Antenna for WLAN Applications**

[4] **FR4 Substrate Datasheet**